7A.5 TESTS OF RANS-BASED PBL SCHEMES AGAINST LES, RUC, AND TALL TOWER DATA

Robert J. Conzemius*
Dennis A. Moon
WindLogics, Inc.
Grand Rapids, Minnesota, USA

1. MOTIVATION

Accurate prediction of first order flow variables in the atmospheric boundary layer relies heavily upon turbulence models, based on Reynolds averaging of the Navier-Stokes equations (RANS), to parameterize the effects of vertical turbulent diffusion on these first order variables. Applications of RANS-based parameterizations include numerical weather prediction (NWP) models, which national meteorological agencies use for forecasting winds. NWP models are also critically important for the rapidly growing wind energy industry, both for purposes of wind resource assessment and for wind forecasts to assist utilities in planning for changes in wind power availability to the electric grid.

One hypothesis central to the application of RANS-based models in NWP is that the turbulent flux of any scalar ϕ is assumed to be proportional to the negative of the vertical gradient of the ensemble average of ϕ,

$$\overline{w'\phi'}(z,t) = -K_\phi(z,t)\frac{\partial\overline{\phi(z,t)}}{\partial z}, \qquad (1)$$

where w is vertical velocity, K_ϕ is a coefficient of diffusivity for ϕ, overbars denote ensemble averages, and primes denote deviations from those averages. For the specific case of the atmospheric boundary layer in NWP, the horizontal average across a grid cell horizontal area can be assumed to be a good substitute for the ensemble average, provided the grid cell horizontal dimensions are large enough.

The flux-gradient hypothesis has its limitations in the atmospheric CBL (Deardorff 1966), particularly with regard to its representation of the effects of CBL-scale turbulence, which has a characteristic depth much larger than the typical grid cell vertical dimension. In such cases, the turbulent vertical motions that must be parameterized extend far beyond adjacent grid cells (often tens of grid cells) in the vertical direction.

In particular, because the relationship (1) must be retained for modeled vertical mixing to occur, the potential temperature gradient is often stronger in the middle CBL than LES or atmospheric measurements would indicate, and because the modeled, middle-CBL potential temperature is less well-mixed in the vertical, the gradient is too weak in the lower CBL. Similar effects are seen with the profiles of velocity components, with (relative to LES) stronger gradients in the middle CBL and weak gradients in the lower CBL (Conzemius 2006).

Two general means to overcome this deficiency have been proposed. The first involves a nonlocal generalization of the flux-gradient relationship (1) (Fiedler 1984),

$$\overline{w'\phi'}(z,t) = \int C(z,z')\frac{\partial}{\partial z'}\phi(z',t)\,dz', \qquad (2)$$

where C is a function describing the potential for mixing between levels z and z'. The relationship (2) is the fundamental basis of transilient turbulence (TT) theory (Stull 1984). The theory has never been widely applied in NWP because of the computational expense of inverting a matrix of mixing coefficients that is often fuller than the typical tridiagonal matrix used for (1), but more recently, Pleim (2007a,b) has devised a more efficient method for solving this type of matrix.

The other method of accounting for the large scale CBL motions is to apply a counter-gradient flux term γ to the diffusion equations,

$$-\overline{w'\phi'}(z,t) = K_\phi(z,t)\left(\frac{\partial\bar{\phi}(z,t)}{\partial z} - \gamma_\phi(t)\right). \qquad (3)$$

The counter-gradient fluxes typically occur in the upper portion of the CBL. Troen and Mahrt (1986) and Hong and Pan (1996) applied this approach to account for counter-gradient fluxes of potential temperature as part of the parameterization that has become known as the medium range forecast model (MRF) PBL scheme. Since then, Noh et al. (2003) and Hong and Pan (2006) have improved the MRF scheme by revising the PBL depth diagnosis criteria, expanding the use of the counter-gradient term to other scalars, and adding an entrainment parameterization. The revised scheme is known as the Yonsei University (YSU) turbulence parameterization. The use of (3) in NWP has the advantage of retaining the numerical simplicity associated with solving a tridiagonal matrix to calculate vertical mixing.

Conzemius (2006) evaluated the transilient approach and compared its predictions of low-level wind and potential temperature profiles to those of the more popular turbulence models employed in NWP. The present study focuses on comparisons between the transilient and counter-gradient approaches for parameterizing the effects of large scale turbulence.

Additionally, we will look at some changes in predicted mean wind speed that arose when we

replaced the MRF PBL scheme by the transilient and the YSU schemes in the NCAR/Penn State MM5 model (Grell et al. 1994). In particular, mean wind speeds were slower in the lowest 2000 meters of the atmosphere than Rapid Update Cycle (RUC) analyses indicated, and they were also slower than tower-measured mean winds speeds. We will investigate the causes behind these reductions in modeled wind speeds.

2. PARAMETERIZATIONS TESTED

2.1. Transilient turbulence based on Richardson number

We tested the Stull (1984) version of the transilient turbulence scheme. In this particular version, the amount of mixing occurring between any two levels *i* and *j* in the model grid is dependent on a bulk Richardson number r_{ij} between those two levels:

$$r_{ij} = \frac{g}{\theta_0} \frac{\Delta z_{ij} \Delta \theta_{ij}}{\Delta u_{ij}^2 + \Delta v_{ij}^2}, \quad (4)$$

where any $\Delta\phi_{ij}$ specifies the change in ϕ between *i* and *j*, *u* and *v* are the *x*- and *y*-components of wind, respectively, θ is potential temperature (θ_o its reference value), and *g* is the gravitational acceleration. The bulk Richardson number is then used to determine a matrix of coefficients, X_{ij},

$$X_{ij} = 1 - w_{ij}\left[1 - \left(\frac{r_{ij}}{R_T}\right)\right], \quad (5)$$

where R_T is a termination value for the Richardson number and was set to be R_T=1. If $r_{ij}>R_T$, X_{ij} is set equal to 1, and there is no mixing between the i^{th} and j^{th} levels. Once turbulence is initiated, it continues until $r_{ij}>R_T$. The weighting factor w_{ij} is given by

$$w_{ij} = \frac{U_0 \Delta t}{(j-i)\delta z}, \quad (6)$$

where U_o is a velocity scale, Δt the time step, and δz is the grid cell vertical dimension. Stull (1984) recommended a velocity scale of U_o=1 m s^{-1}. However, we used U_o=0.25$(B_s z_i)^{1/3}$, where B_s is the surface buoyancy flux, and z_i is the boundary layer depth. The boundary layer depth z_i was defined as the level where the buoyancy flux reaches its minimum in the entrainment zone. The proposed U_o is the Deardorff (1970) convective velocity scale multiplied by a reduction factor of 0.25 in order to keep vertical gradients in the mid-CBL from becoming smaller than those simulated using LES.

The exchange coefficients c_{ij} were then calculated using the constraint

$$\sum_{k=1}^{j-1} c_{ik} - (j-1)c_{ij} = X_{ij}; \quad i < j. \quad (7)$$

The factor *j*-1 is applied so that the mixing is more intense near the ground and is reduced at higher levels. The diagonal elements are then calculated so that each row in the exchange matrix sums to unity, and the matrix c_{ij} is symmetrized to ensure conservation of state and mass. It should be noted that a symmetric matrix forces the transilient scheme to obey the same flux-gradient relationship (1) used in the other turbulence closures, but its nonlocal formulation allows scalar vertical gradients to approach zero in the mid-CBL more closely than would the case with local formulations.

The change of values of the scalar $\phi_.$ due to turbulent mixing, from time step *n* to time step *n*+1 is then calculated according to the formula

$$\phi_i^{n+1} = \phi_i^n + c_{ij}\phi_j^n. \quad (8)$$

The Prandtl number is assumed to be unity. That is, the same matrix c_{ij} is used for the exchange of all scalars in the CBL. The time tendency of $\phi_.$ is

$$\frac{\partial \phi_i}{\partial t} = \frac{\phi_i^{n+1} - \phi_i^n}{\Delta t}. \quad (9)$$

In our application of the transilient model, the non-local Richardson number r_{ij} was truncated to fall between r_{ij}=0 and $r_{ij}=R_T$. The r_{ij}=0 truncation removes occurrences of very large negative r_{ij} when the shear is near zero and the vertical potential temperature gradient is only slightly negative. Such situations can result in unreasonably large variations in X_{ij} when the stability of the atmosphere between *i* and *j* is near neutral. The $r_{ij}=R_T$ truncation had the same effect as truncating X_{ij} to be no greater than X_{ij}=1.

2.2. YSU PBL parameterization

The YSU PBL parameterization is more fully described in Hong et al. (2006) and Noh et al. (2003). The underlying principle of this nonlocal scheme is that the turbulence can be scaled by a length scale equal to the boundary layer depth and by a velocity scale that is a combination of the Deardorff (1970) velocity scale $w_* = (B_s z_i)^{1/3}$ for the CBL and the friction velocity u_*. The exchange coefficients in the PBL are specified according to a self-similar profile that is scaled to the PBL depth.

The PBL depth is diagnosed using a Richardson number criterion, which is evaluated starting at the lowest model level.

$$\mathrm{Ri}_B = \frac{gz}{\theta_{v,1}} \frac{(\theta_{v,k} - \theta_{v,1})}{(u_k^2 + v_k^2)}, \quad (10)$$

where θ_v is virtual potential temperature, *z* is the height above ground level, the subscript 1 refers to the lowest model level above ground, and the subscript *k* refers to the k^{th} model level. The wind speed is constrained to $(u_k^2 + v_k^2) \geq 1$ to prevent unreasonably large values of Ri_B from being evaluated numerically. The level at which Ri_B first becomes greater than zero is defined at the height of the top of the PBL, z_i.

Preliminary tests against LES data showed that the profile of exchange coefficients could be further tuned to match the LES profile (see section 3). Additionally, initial test results in MM5 modeling exercises showed some differences between

modeled wind speeds and measured wind speeds in the nocturnal PBL. Banta et al. (2006) made arguments for decreasing the exchange coefficients in the nocturnal PBL because the models are unable to predict the wind speed maximum and the relatively low height of the nocturnal low-level jet.

Motivated by these findings, we decided to modify the YSU parameterization in an attempt to improve the surface layer wind speed predictions. Since many PBL parameterizations are based on the theory that the exchange coefficient can be calculated using an *e-l* type relationship, where *e* is turbulence kinetic energy (TKE) and *l* is a length scale of turbulence, we decided to employ a length-scale-based adjustment of the vertical exchange coefficients near the lower surface. For stable conditions, we defined a buoyancy length scale

$$l_b = 3.4\left(\frac{K_h}{N}\right)^{1/2}, \qquad (11)$$

Where K_h is the eddy exchange coefficient for heat, and N is the Brunt-Väisälä frequency. A net length scale was defined as

$$l_n = \frac{1}{\left(\frac{1}{z_q}+\frac{1}{l_b}\right)}, \qquad (12)$$

where z_q is the above-ground height of the top of the grid cell being evaluated. The exchange coefficients are then multiplied by a factor of

$$x_f = \left(\frac{l_n}{l_b}\right)^{1.5} \qquad (13)$$

for all cases in which the conditions are stable. The effect of x_f is to limit exchange coefficients in cases when the turbulence length scale should be limited by distance from the ground.

During the day, a profile of eddy exchange coefficients K is normally calculated in the YSU scheme using the formula

$$K = K_o + w_m \kappa z\left(1-\frac{z-z_s}{z_i-z_s}\right)^2, \qquad (14)$$

where K_o is a minimum value that depends on the depth of the grid cell, $w_m = \left[u_*^3 + 8\kappa w_*^3 (z/z_i)\right]^{1/3}$ is a velocity scale characteristic of the CBL (Noh et al. 2003), κ is the von Karman constant, z is the height above ground level, z_s is the height of the center of the lowest model half sigma level, and z_i is the CBL depth. This relationship was modified to

$$K = K_o + 2w_m \kappa z\left(\frac{z}{z+70}\right)\left(1-\frac{z-z_s}{z_i-z_s}\right)^3, \qquad (15)$$

resulting in an effective reduction of length scale in the surface layer but increasing the mixing just above the surface layer. The change of exponent on the far right side also changes the profile throughout the depth of the PBL.

Additionally, a limit was imposed on the entrainment velocity w_e in the scheme:

$$w_e \le \frac{z_i}{\Delta t}, \qquad (16)$$

where Δt is the model time step. Imposing this limit in the code prevented the CFL crashes in MM5 that occurred with the original version of the YSU PBL parameterization.

3. LARGE EDDY SIMULATION CASES

Large eddy simulation data were used to tune the parameterizations as specified in section 2. Because large eddy simulation resolves most of the energy-containing motions in the turbulent flow, it is a useful tool for performing tests of RANS-based turbulence closures under idealized testing conditions. LES experiments can be designed to focus on one or more particular mechanisms governing the evolution of the CBL while excluding other competing mechanisms. A set of 24 CBL experiments was used for this tuning. The details of these experiments can be found in Conzemius and Fedorovich (2006). They can be briefly summarized by describing two of the basic configurations of atmospheric flow:

1. No mean shear (**NS** case), which was the reference case.
2. Height-constant geostrophic wind of the 20 m/s magnitude throughout the whole simulation domain (**GC** case).

For all simulated cases, the surface roughness length, geographic latitude, and reference temperature were prescribed to be 0.01 m, 40° N, and 300 K, respectively. Although the **NS** case has no wind, the purpose of including such a case in the present study is to allow the testing to utilize a variety of CBL conditions ranging from a purely convective CBL (NS) to a shear-driven CBL (GC). We thereby hope to add the greatest possible generality to the results.

The virtual potential temperature θ changed vertically at a constant rate of 0.001, 0.003, or 0.010 K/m throughout the entire domain starting from the surface. The initial wind velocity in the domain was geostrophic (zero in the **NS** case), with the vertical velocity component set equal to zero. The surface heat flux had values of 0.03, 0.10, or 0.30 K m s^{-1} and was kept constant with time throughout the run.

The evaluation of the turbulence closures was carried out in a similar manner to Moeng and Wyngaard (1989) and Ayotte et al. (1996). The LES code was reduced to a one-dimensional column model, and the turbulence closure schemes described in section 2 were inserted into the code. The code was then run for the same period of time as in the LES cases, using the same vertical resolution as the LES grid, and vertical profiles were extracted from the model at a period of time considered to be representative of the CBL evolution.

Figure 1 shows an example of the results of these LES tests. Initial results from tests of the modified YSU PBL scheme revealed that the YSU PBL profile matches LES results more closely than the TT profile did, particularly in the upper portion of

the CBL, where the TT parameterization performed relatively poorly (but still better than MRF). For purposes of comparison, the original MRF PBL turbulence parameterization results are plotted alongside those of TT and YSU. The relatively poor results of the MRF scheme are mostly due to the use of a larger critical bulk Richardson number of Ri_B=0.5 for the diagnosis of the PBL depth, resulting in excessively deep PBL diagnoses for the GC case and consequent mixing over too deep a layer. The YSU scheme uses a smaller critical value of Ri_B=0, and its diagnoses of CBL depth are more realistic compared to LES.

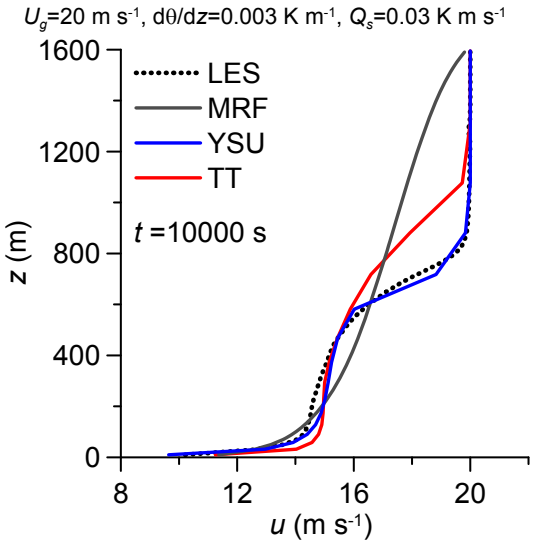

Figure 1. Profiles of the *x*-component of wind predicted by turbulence closure schemes and LES for the GC case at *t*=10000 s with a surface heat flux of 0.03 K m s^{-1} and a vertical potential temperature gradient of 0.003 K m^{-1}.

4. TESTS IN MM5 VERSUS TOWER DATA

We incorporated the YSU and TT PBL schemes into the MM5 model and tested them against meteorological tower data at two sites in the central U.S. The first site is located in the southern Plains, where the wind resource is dominated by the presence of a southerly nocturnal low-level jet in the summer. The characterization of the low-level jet is highly dependent on the representation of boundary layer dynamics as well as the distribution of heating and cooling between the Rocky Mountains to the west and the Mississippi River Valley to the east. The second site is near the town of Summit, which is located in northeastern South Dakota. The low-level jet contributes to the wind climate there during the summer, but the greater influence comes from larger (synoptic) scale cyclones and anticyclones.

For both sites, the MM5 model was run for a period of one year utilizing RUC hourly analyses as initial and boundary conditions. Generally, the runs were started at the beginning of each month and allowed to proceed continuously until the end, but for the Summit South Dakota site, each month was divided into two separate runs. For the southern Plains site, a 30 km outer grid with dimensions of 60×60×35 was used. A 10 km, 51×51 grid was nested inside the outer grid. For the Summit, South Dakota location, an 18 km outer grid with dimensions of 60×60×35 was used. Two nested inner grids (6 km and 2 km) had dimensions of 60×60 and 51×63, respectively. All grids had 35 vertical levels, with the lowest half-sigma level located approximately 10 meters AGL.

In order to calculate predicted wind statistics, MM5 data were output once per hour, and wind data were extracted from the innermost grid of MM5 at the same levels as the tower measurements. For the southern Plains site, the anemometer heights were 30 m, 50 m, and 70 m AGL, and for the Summit, South Dakota location, anemometer heights were 50 m and 70 m AGL. Monthly and annual average wind speeds were calculated from the hourly values, and the diurnal wind speed cycle was calculated for each month separately.

5. RESULTS OF MM5 TESTS

The diurnal cycle of wind speeds provides one of the better indications of the ability of a particular turbulence parameterization to represent boundary layer processes. These profiles can be evaluated in terms of overall wind speed, magnitude of the diurnal cycle, and wind shear (difference between the two levels plotted for each location).

One of the most apparent differences between the MRF and the other two parameterizations at the Southern Plains site (Fig. 2) is the amplitude of the diurnal cycle. This is somewhat evident in January, but it is much more pronounced in August, when the diurnal forcing is a bit stronger. The general behavior among all three parameterizations, however, is qualitatively the same. At night (0000 UTC to 1200 UTC), the MRF has faster wind speeds than the other two parameterizations, but during the day, the MRF-predicted wind speeds are slower than both the tower observations as well as the other parameterizations.

A closer examination of the wind speed profiles shows that the MRF predicts excessively deep PBLs, which is a behavior that has been noted in other studies (e.g. Berg and Zhong 2005). This behavior causes the wind speeds to decrease during the day because of excessive mixing of slower speeds, both from below and from above, into the layer occupied by the low-level jet.

At night, the faster wind speeds are the result of a mismatch caused by using two separate methods for calculating mixing coefficients. In the PBL, the mixing coefficients are calculated according to the nonlocal formulation (14), but above the PBL top, the mixing coefficients are calculated using a local Richardson number-based formula (see Fig. 3). The result of the mismatch is an anomalously strong and shallow nocturnal low-level jet, which is quickly mixed

out during the day. The problem is fixed by decreasing the value of the critical Richardson number, used to diagnose the PBL depth, from 0.5 to 0, as is done in the YSU parameterization, so that in stable (nighttime) conditions, the YSU scheme diagnoses a PBL depth near zero and uses the local Richardson number approach throughout the entire column depth.

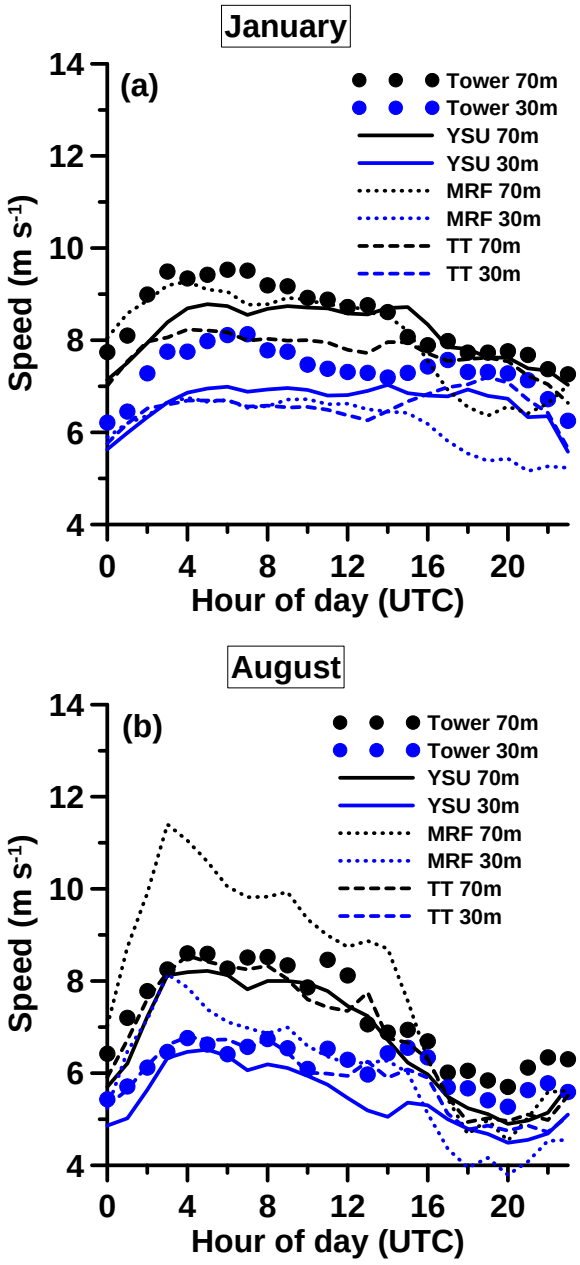

Figure 2. Diurnal cycle of wind speeds for Southern Plains site for (a) January 2004; and (b) August 2004.

The shear between z=30m and z=70m is quite large for MRF, and the TT scheme seems to predict too little shear during the day when compared to tower observations. Otherwise, the TT scheme exhibits reasonable shear at night, and the YSU scheme may have the best overall characterization of shear between these two levels.

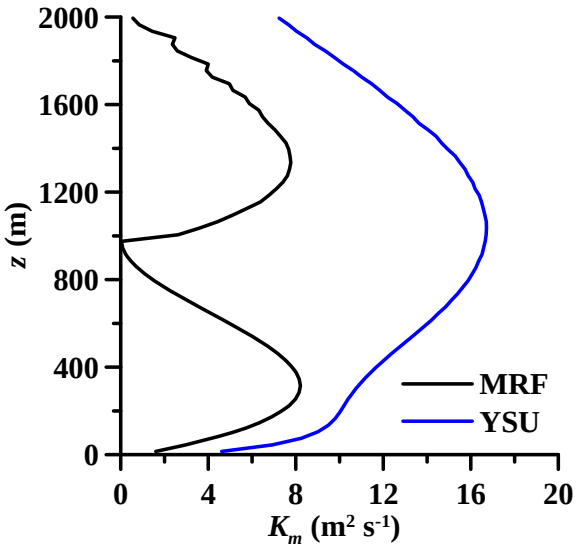

Fig. 3. Example of nighttime profiles of momentum exchange coefficents for the MRF and YSU parameterizations.

At the Summit, South Dakota site, some of the same characteristics of the three schemes are present (Fig. 4) as were found at the Southern Plains site. In January (Fig. 4a), all schemes produce very similar looking diurnal wind speed cycles. However, in April, when the diurnal cycle is more pronounced, the MRF shows its characteristic bias of large wind speeds at night. At this particular site in April 2004, however, the MRF speeds match the tower data more closely than do the predicted speeds of the other two parameterizations.

The TT and YSU schemes may provide a better representation of the diurnal cycle than MRF (with the exception of Fig. 4b), but they predict a smaller annual average wind speed. At the southern plains site, MM5 with the MRF parameterization predicts the fastest annual average wind speeds. The MRF parameterization also more accurately predicts average wind speeds on a month by month basis (Fig. 5). The faster MRF-predicted wind speeds at the tower levels are, however, an artifact of the mischaracterization of the nocturnal low-level jet. Removing this problem reveals that the MM5-predicted low-level jet is too weak over much of its depth. This under-prediction of speed is compensated by the over-prediction of speed in the lowest couple hundred meters above ground, so when speeds are extracted at tower heights, it appears the low-level jet strength is excessive, whereas in an integral sense (over the depth of the entire layer), it is slow.

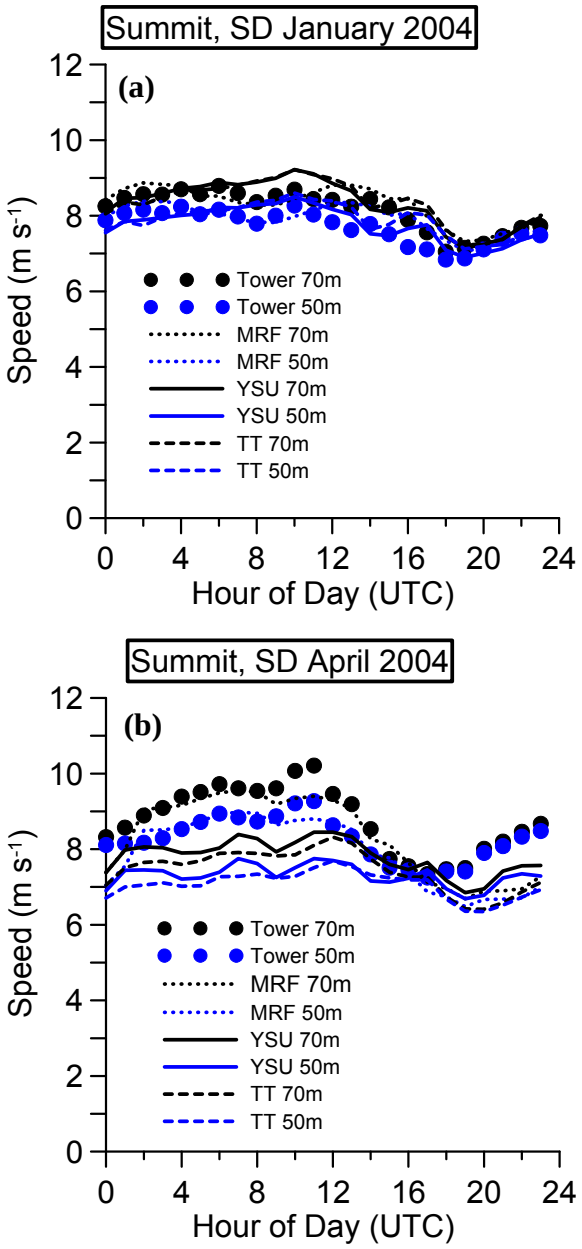

Figure 4. Diurnal cycle of wind speeds for Southern Plains site for (a) January 2004; and (b) April 2004.

Table 1. Annual Average Wind Speeds

Location	Level (m)	Wind Speed (m s^{-1})			
		MRF	TT	YSU	Tower
Southern Plains	70	8.63	7.64	7.82	8.08
	30	6.52	6.47	6.31	7.23
Summit*	70	8.87	8.48	8.81	8.93
	50	8.40	8.01	8.18	8.12

*Annual averages for Summit exclude the month of August because no tower data were available possible for that month.

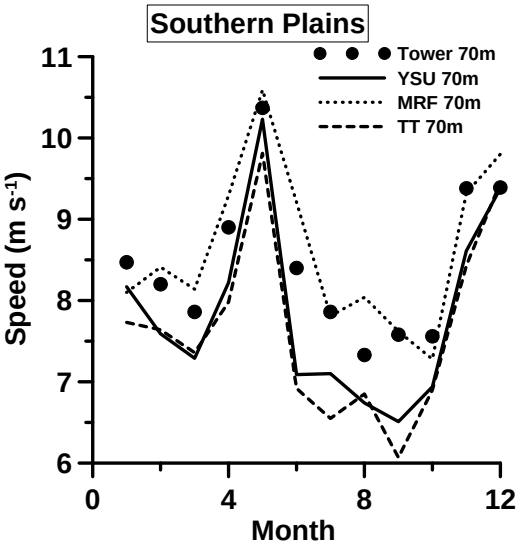

Fig. 5. Monthly average wind speeds predicted by MM5 with the YSU, MRF, and TT parameterizations at *z*=70 m AGL compared to tower observations.

MM5-predicted wind speeds were compared to RUC-analyzed wind speeds over the outer grid, and it was found that the speed bias exists over much of the MM5 domain (Fig. 6). Since RUC is used as lateral boundary conditions, the calculated bias is zero around the edges of the domain. However, over much of Texas, there is a rather substantial layer where the predicted flow is slower than in the RUC analyses. The flow in the interior domain represents a substantial deviation from RUC because the lateral boundary conditions are taken from RUC.

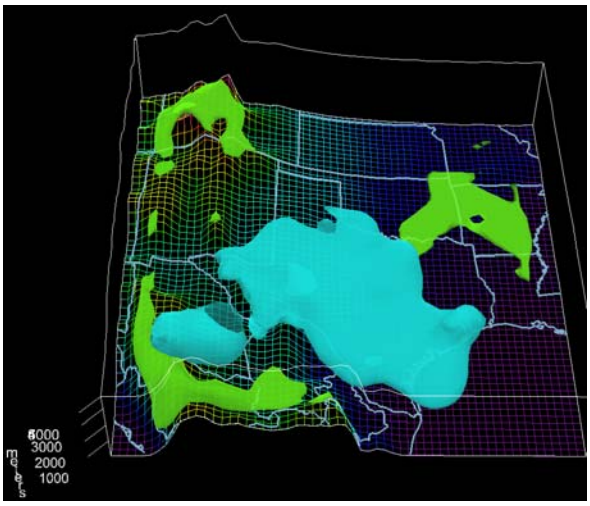

Fig. 6. Isosurfaces of MM5 v3.70a wind speed bias (versus RUC analyses) for the Month of July 2004. The blue-green isosurfaces denote a bias of –2 ms^{-1} and the green-yellow isosurfaces denote the +2 m s^{-1} bias.

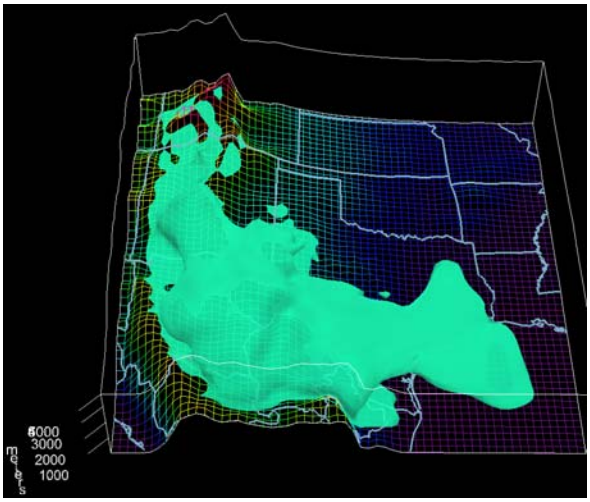

Fig. 7. Isosurface of MM5 v3.70a –2.0 K temperature bias at for the Month of July 2004.

Further investigation into the mechanisms for the deviation have revealed that there is also a relatively deep temperature bias that develops over the Rocky Mountains and the Gulf coast (Fig. 7). The cold bias extends upward from the surface through at least the lowest 2000 meters of the atmosphere. This finding motivated an additional experiment to investigate the effects of choosing a different scheme for representing the land-atmosphere energy balance. The MM5 ISOIL option was changed from the six-layer soil model (ISOIL=1) to the Noah land surface model (ISOIL=2), and MM5 was rerun with the YSU parameterization for both the Southern Plains and Summit, South Dakota test locations.

Table 2. LSM Wind Speed Comparison at Southern Plains Site

	Speed (m/s)			Errors	
	Tower	LSM	YSU	LSM	YSU
Jan	8.49	8.41	8.17	-1%	-4%
Feb	8.28	7.80	7.59	-6%	-8%
Mar	7.92	7.43	7.29	-6%	-8%
Apr	8.83	8.41	8.22	-5%	-7%
May	10.43	10.40	10.23	0%	-2%
Jun	8.37	9.06	7.09	+8%	-15%
Jul	7.97	8.00	7.10	0%	-11%
Aug	7.30	7.90	6.74	+8%	-8%
Sep	7.59	7.26	6.51	-4%	-14%
Oct	7.61	7.51	6.94	-1%	-9%
Nov	9.34	9.09	8.61	-3%	-8%
Dec	9.77	9.52	9.38	-3%	-4%
AVG	8.49	8.40	7.82	-1%	-8%
MAE		0.31	0.67	4%	8%

Table 2 shows the comparison between LSM and nonLSM versions of MM5. With the Noah LSM option chosen, MM5-predicted wind speeds match tower observations much more closely.

Comparison with RUC analyses shows that the negative wind speed biases over the southern Plains using the LSM option are much smaller than with the 6-layer soil option. Overall, the strength and depth of the low-level jet appears to be reproduced much more adequately.

Tests of the 6-layer soil model against the Noah LSM model at the Summit, South Dakota site do not show a significant difference between the ability of MM5 to predict the wind speeds at that site with either option. It appears the Noah LSM option has a larger impact on MM5-predicted wind speeds over the south-central part of the U.S. where the low-level jet is dependent on the accurate characterization of the gradients in heating between the higher terrain to the west and lower terrain to the east.

6. CONCLUSIONS

The transilient turbulence (TT) parameterization evaluated provides an improvement over the medium range forecast model (MRF) parameterization in terms of reproducing the evolution of mean first order profiles and bulk boundary layer characteristics such as PBL depth. The Yonsei University (YSU) parameterization, which is an extensive revision to the MRF parameterization, predicts the best overall evolution of CBL characteristics compared to LES. In particular, the YSU compares more favorably against LES in the upper CBL. The layer of countergradient flux, typically seen in the upper portion of the CBL can be reproduced by YSU whereas, in the particular version of the transilient turbulence parameterization investigated in the present paper, countergradient flux is not possible.

In tests of these schemes in MM5 against tall tower data, the TT scheme and the YSU scheme appear to produce similar wind speeds, but, the smaller computational expense of the YSU scheme gives it a great advantage over TT when used in numerical weather prediction. For the YSU scheme in particular, we find that its improvement over the older MRF parameterization can be attributed primarily to the change in critical value of the Richardson number, which was decreased from 0.5 to 0, to diagnose the PBL depth. This change has two primary effects. During the day, the depth of the mixing is reduced to that which would occur mostly due to buoyancy effects. In the stably stratified nocturnal PBL, the Ri_B=0 criterion ensures that the nonlocal formulation is never used, eliminating the mismatch that occurs between nonlocal and local formulations of exchange coefficients.

We have found that it is necessary to provide a limit on the entrainment parameterization that is used in the YSU scheme in order to avoid numerical instabilities. Although the particular instance of such instabilities in our case was due largely to poorly

initialized low-level velocity fields, providing a limit will eliminate the possibility of unrealistic amounts of entrainment.

It is important to correctly model the land surface-atmosphere energy balance to accurately predict the speed and depth of the low-level jet, which is a response to the heating gradients provided by the elevated heat source (Rocky Mountains) to the west of the study locations. One could certainly expect that this would also be the case for thermally driven flows, such as sea breezes, as well.

7. REFERENCES

Ayotte, K. W., P. P. Sullivan, A. Andren, Scott C. Doney, A. A. M. Holtslag, W. G. Large, J. C. McWilliams, C.-H. Moeng, M. J. Otte, J. J. Tribbia, and J. C. Wyngaard, 1996: An evaluation of neutral and convective planetary boundary-layer parameterizations relative to large eddy simulations. *Bound. Layer Meteorol.,* **79,** 131-175.

Banta, Robert M., L. Mahrt, D. Vickers, J. Sun, B. B. Balsley, Y. L. Pichugina, and E. J. Williams, 2006: Shallow boundary layers and suppressed vertical mixing in the very stable boundary layer with a weak LLJ, Preprints, *17th Symp. on Boundary Layers and Turbulence*, Amer. Meteor. Soc., 21-25 May, San Diego, California, USA, CD-ROM, J1.5.

Berg, L. K., and S. Zhong, 2005: Sensitivity of MM5-simulated boundary layer characteristics to turbulence parameterizations. *J. Applied Meteor.,* **44,** 1467-1483.

Conzemius, R. J., 2006: Tests of transilient versus flux-gradient turbulence parameterizations for the prediction of surface layer wind profiles. Preprints, *17th Symp. on Boundary Layers and Turbulence*, Amer. Meteor. Soc., 21-25 May, San Diego, California, USA, CD-ROM, 9.3.

Conzemius, R. J., and E. Fedorovich, 2006: Dynamics of sheared convective boundary layer entrainment. Part I: methodological background and large eddy simulations. *J. Atmos. Sci.,* **63,** 1151-1178.

Deardorff, J. W., 1966: The Counter-Gradient Heat Flux in the Lower Atmosphere and in the Laboratory. *J. Atmos. Sci.,* **23,** 503–506.

Deardorff, J. W., 1970: Convective velocity and temperature scales for the unstable planetary boundary layer and for Raleigh convection. *J. Atmos. Sci.*, **27**, 1211-1213.

Fiedler, B. H., 1984: An integral closure model for the vertical turbulent flux of a scalar in a mixed layer. J. Atmos. Sci., 41, 674-680.

Grell, G. A., J. Dudhia, and D. R. Stauffer, 1994: A description of the Fifth-generation Penn State/NCAR mesoscale model (MM5). NCAR Technical Note, NCAR/TN-98+STR, 117 pp.

Hong, S.-Y., and H.-L. Pan, 1996: Nonlocal Boundary Layer Vertical Diffusion in a Medium-Range Forecast Model. *Mon. Wea. Rev.,* **124,** 2322–2339.

Hong, S.-Y., Y. Noh, and J. Dudhia, 2006: A new vertical diffusion package with an explicit treatment of entrainment processes. *Mon. Wea. Rev.,* **134,** 2318-2341.

Moeng, C.-H. and J. C. Wyngaard, 1989: Evaluation of turbulent transport and dissipation closures in second-order modeling. *J. Atmos. Sci.,* **46,** 2311-2330.

Noh, Y., W. G. Cheon, S. Y. Hong, and S. Raasch, 2003: Improvement of the K-profile model for the planetary boundary layer based on large eddy simulation data. *Bound.-Layer Meteor.,***107,** 401–427.

Pleim, J. E., 2007: A combined nonlocal closure model for the atmospheric boundary layer. Part I: model description and testing. *J. Appl. Meteor. and Climatol.,* **46,** 1383-1395.

Pleim, J. E., 2007: A combined nonlocal closure model for the atmospheric boundary layer. Part II: application and evaluation in a mesoscale meteorological model. *J. Appl. Meteor. and Climatol.,* **46,** 1396-1409.

Stull, R. B., 1984: Transilient turbulence theory. Part I: the concept of eddy-mixing across finite distances. *J. Atmos. Sci.,* **41,** 3351-3367.

Troen, I., and L. Mahrt, 1986: A simple model of the atmospheric boundary layer; sensitivity to surface evaporation. *Bound.-Layer Meteor.,* **37,** 129-148.